

Multi-band Vector Wavelet Transformation based Multi-Focus Image Fusion Algorithm

Yihua Lan, Haozheng Ren, Yong Zhang

School of Computer Engineering, Huaihai Institute of Technology, Lianyungang, China
lanhua_2000@sina.com, renhaozheng666@163.com, zhyhglyg@126.com

Chih-cheng Hung*

School of Computing and Software Engineering, Southern Polytechnic State University, Marietta, USA
Chung2012@sina.com

Abstract—Multi-focus image fusion is one of the important embranchments of image fusion. It has been widely used in target identification, remote sensing image processing and so on. In this paper, a new multi-focus image fusion method based on multi-band vector wavelet is presented. Furthermore, some post processing is done in this paper, in which anisotropic diffusion arithmetic based on partial differential equations is used. As for the fusion image, the blocking effects which usually existed in the results are eliminated by using wavelet based image fusion method. To test and evaluate the proposed method, it is applied to a case study to demonstrate its performance in image fusion. Comparisons of experimental results by using several methods demonstrated the effectiveness of our proposed methods.

Index Terms—Image fusion, Wavelet analyses, Multi-band vector wavelet, Diffusion equation, Blocking effects, Image Enhancement, Diffusion Equation, Post filtering

I. INTRODUCTION

Imaging cameras, like human eyes, usually have only a finite depth of field, especially those with long focal lengths. It means that in those images which are captured by these cameras, only those objects or scenes within the depth of field of the camera are focused, while others are blurred [1]. An image that is in focus everywhere contains more information than the one which is focused on one object or limited scenes within the depth of field of the camera [2]. To obtain an image with every object in focus, we usually use the techniques of image fusion to produce an image with an extended depth of field by employing a series of images taken from the same view point under different focal settings.

Image fusion has become an important issue in image analysis and computer vision area during the last decade [3], which aims to integrate complementary and redundant information from two or more images of a scene or taken from different sensors into a highly informative image, which contains a ‘better’ description

of the scene than any of the individual source images, and is more suitable for human and machine perception, or further image-processing tasks such as segmentation, feature extraction and object recognition. Thus, this technique plays important role in many fields such as computer vision, biomedical imaging, and remote sensing etc. Multi-focus image fusion is a key research field of image fusion (1). It is a technique that obtains a completely clear image, which is the same image setting or the same scene but with different focus points. The work area of image fusion is divided into spatial domain, spectral domain, and frequency domain and domain-scale integration. On the other side, depending on the merging stage from low to high, multi-focus image fusion is usually performed at one of the three different processing levels: pixel-level, feature-level and decision-level [4]. The pixel level fusion concerns the aggregation of the raw data provided directly from multi-focus images. It takes the averages of the source images pixel by pixel, and has been the most frequently considered in most literature. It is a very important and key technique. This paper will mainly address the problems of pixel level image fusion. The relevant pixel level fusion schemes can be categorized into space domain and transform domain. The fusion algorithms in space domain, including logic filtering algorithms, arithmetic algorithms and partition fusion algorithms, produces the fused image pixel by pixel directly, without any transformation [5]. In transform domain, fusion algorithms always decompose input images at various resolutions, fuse individual or groups of pixels from the multi resolution pyramid representations with different schemes [6].

In recent years, a number of researchers recognized that multi-scale transforms are very useful for analyzing the information content of images for the purpose of fusion [7-9]. Commonly used multi resolution transformations include the Laplacian pyramid [7], gradient pyramid [8], and wavelet transform (WT) [9]. As a kind of pixel level fusion method, WT, with its properties of multi-resolution and multi-scale analysis, is currently being widely used in image fusion technology, which has been a recent research focus among several proposed solutions. However, traditional WT has some

Manuscript received May 28, 2012; revised June 1, 2012; accepted July 16, 2012. *Corresponding author.

disadvantages such as not having some simultaneous properties. In this paper, we propose a new multi-focus image fusion algorithm based on multi-band vector wavelet transform. Furthermore, considering the image blocks effect, a post-processing is proposed to enhance the visual Effects.

The paper is organized as follows: A review of the wavelet based multi-focus image fusion method is presented in Section 2. In section 3, we present the proposed algorithm. Experiments with the proposed approach and comparison with other existing methods can be found in Section 4, and performance of the evaluation methods is also described in this section. Section 5 presents the conerning discussion. In the final Section 6, the conclusion of whole paper is drawn.

II. WAVELET BASED MULTI-FOCUS IMAGE FUSION METHOD ANALYSIS

The wavelet transformation, which is a mathematical tool, could detect local features in a signal process. It can also be used to decompose two-dimensional gray-scale image signals into different resolution levels for multi resolution analysis. Over the past decades, a significant amount of researches have been conducted concerning the application of wavelet transforms in image fusion. Wavelet analysis has been greatly successful in the area of image fusion.

Generally speaking, the WT based image fusion method firstly performs multi resolution decomposition on all source images respectively. Then the coefficients can be calculated by using a certain fusion rule. At last, the method is used to perform the inverse WT with the corresponding coefficients, and the fused image is obtained. Figure 1 illustrates this process. Therefore, the detailed fusion steps based on WT can be described as follows:

Step 1: All source images are processed with multi resolution decomposition based on WT. One thing should be noticed is that the result images with m-level decomposition includes one low frequency portion and 3m high frequency portions.

Step 2: By using a certain fusion rule, the coefficients of different portions can be obtained.

Step 3: The ultimately fused image is reconstructed with the combined transform coefficients from step 2 by performing the inverse WT.

It should be noticed that all source images to be fused must be registered at first to assure the corresponding pixels are aligned.

With the development of the WT technique, WT provides better image fusion performance than pyramid algorithms because of its orthogonality, symmetry and compact support. The WT of image signals produces a non-redundant image representation, it provides better spatial and spectral localization of image information compared with other multi resolution representations. However, still some problems that should be addressed in WT. The first one is that the 2-band WT may process effectively the case of resolution difference with 2i times, but it may obtain some poor effects in other cases. The

second one is that the multi level WT only decomposes the low frequency bands with different levels, which may cause a larger scaling coefficient, worse local characteristics of spectral, and coarser spectral resolution. The third one is that with wavelet decomposition scale increasing, there will be obvious blocking effects in fused image, and the spectral information of the fused image will be lost increasingly. Focusing on these problems, we propose some methods to address them in our novel fusion method.

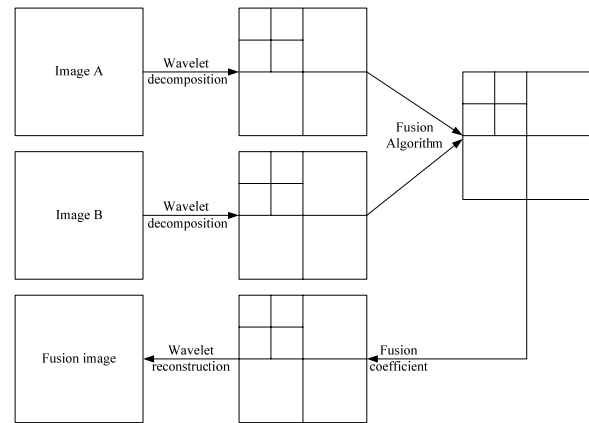


Figure 1. Image fusion based on traditional wavelet decomposition and reconstruction method

III. THE PROPOSED IMAGE FUSION METHOD

In this section, the techniques used in the proposed method and the reasons for the blocking effect in the fused image are analyzed, then the detailed descriptions of the whole proposed method are given.

A. Multi-band Wavelet Analysis

Applications of wavelet analysis are potentially extensive, and the technique has been used in many different scientific and application fields successfully. On the contrary, the improvement of wavelet theory itself is actually further contributed by these applications. As a result, many new branches such as multi-band wavelet transformation have appeared [10].

The multi-band wavelet can be considered as a more generic case of the two-band wavelet transformation. A multi-band wavelet ($M > 2$) is superior to two-band wavelet in many aspects, including compact support, orthogonal aspects, and especially in its decomposition characteristics. A brief introduction to the orthogonal Multi-band wavelet transform is given as follows.

Giving $\{\mathbf{V}_j\}$, $\phi(x)$, $\{\psi_s(x), 1 \leq s \leq M - 1\}$ is Multi-band wavelet function.

Assuming

$$\phi_{j,k}(x) = M^{j/2} \phi(M^j x - k),$$

$$\psi_{j,k}^s(x) = M^{j/2} \psi^s(M^j x - k), 1 \leq s \leq M - 1,$$

and $f_{j+1} \in \mathbf{V}_{j+1}$ is $f(x)$ orthogonal transformation on space \mathbf{V}_{j+1} , $f_{j+1}(x) = \sum_{k \in \mathbf{Z}} a_{j+1,k} \phi_{j+1,k}(x)$, hence,

$$f_{j+1} = f_j + g_j = f_j + \sum_{s=1}^{M-1} g_j^s.$$

The decomposition algorithm can be expressed as follows:

$$\begin{aligned} \langle \phi_{j+1,k}, \phi_{j,l} \rangle &= c_{k-Ml}, \langle \phi_{j+1,k}, \psi_{j,l}^s \rangle = d_{k-Ml} \\ &1 \leq s \leq M-1; \\ f_j &= \sum_{k \in \mathbf{Z}} a_{j,k} \phi_{j,k}(x), g_j^s = \sum_{k \in \mathbf{Z}} b_{j,k}^s \psi_{j,k}^s(x) \\ &1 \leq s \leq M-1; \\ a_{j,k} &= \sum_{n \in \mathbf{Z}} c_{n-Mk} a_{j+1,n}, b_{j,k}^s = \sum_{n \in \mathbf{Z}} d_{n-Mk}^s a_{j+1,n} \\ &1 \leq s \leq M-1. \end{aligned} \quad (1)$$

The corresponding reconstruction algorithm is

$$a_{j+1,k} = \sum_{n \in \mathbf{Z}} \left(c_{k-Mn} a_{j,k} + \sum_{s=1}^{M-1} b_{j,k}^s d_{k-Mn}^s \right) \quad (2)$$

For $f(x, y) \in L^2(\mathbf{R}^2)$, decomposition and reconstruction of Multi-band wavelet are

$$\begin{aligned} a_{j,k,l} &= \sum_m \sum_n c_{m-Mk} c_{n-Ml} a_{j+1,m,n} \\ b_{j,k,l}^{t,s} &= \begin{cases} \sum_m \sum_n c_{m-Mk} d_{n-Ml}^s a_{j+1,m,n} & (t=0, 1 \leq s \leq M-1) \\ \sum_m \sum_n d_{m-Mk}^t c_{n-Ml} a_{j+1,m,n} & (1 \leq t \leq M-1) \\ \sum_m \sum_n d_{m-Mk}^t d_{n-Ml}^s a_{j+1,m,n} & (1 \leq t, s \leq M-1) \end{cases} \end{aligned} \quad (3)$$

$j = 0, 1, 2, \dots, \{a_{j,k,l}\}$ is the j level low frequency, $\{b_{j,k,l}^{t,s}\}$ are the j level high frequency.

The Multi-band WT of a 2-dimensional signal includes one low frequency portion and $M^2 - 1$ high frequency portions. The reconstruction algorithm is described as follows:

$$\begin{aligned} a_{j+1,k,l} &= \sum_m \sum_n c_{k-Mm} c_{l-Mn} a_{j,k,l} \\ &+ \sum_{t,s=0, s+t \neq 0}^{M-1} \sum_m \sum_n d_{k-Mm}^t d_{l-Mn}^s b_{j,k,l}^{t,s} \end{aligned} \quad (4)$$

B. Vector Wavelet Analysis

Vector wavelet was first proposed by Goodman et al. [11]. By introducing several analysis and synthesis operators, Vector wavelet decompositions offer more design flexibility, and has some advantages over scalar wavelets in relation to properties which are known to be important in signal processing such as short support,

orthogonality, symmetry, and vanishing moments. A scalar wavelet cannot possess all these properties at the same time, whereas a vector wavelet can provide perfect reconstruction simultaneously [12]. The vector wavelet multi-resolution analysis is described as follows. Assuming

$$\begin{aligned} \Phi(x) &= (\phi_1(x), \phi_2(x), \dots, \phi_N(x))^T \in L^2(\mathbf{R})^N, \\ \phi_l(x) &\in L^2(\mathbf{R}), l = 1, \dots, N. \end{aligned}$$

The multi-resolution analysis space can be expressed as follows

$$\mathbf{V}_j = \overline{\text{span}\{M^{j/2} \phi_l(M^j x - k) : 1 \leq l \leq N, k \in \mathbf{Z}\}}$$

If \mathbf{V}_j satisfies the following conditions:

- (1) $\dots \subset \mathbf{V}_{-1} \subset \mathbf{V}_0 \subset \mathbf{V}_1 \subset \dots$;
- (2) $\overline{\bigcup_{j \in \mathbf{Z}} \mathbf{V}_j} = L^2(\mathbf{R})$; $\bigcap_{j \in \mathbf{Z}} \mathbf{V}_j = 0_{N \times 1}$;
- (3) $f(x) \in \mathbf{V}_j \Leftrightarrow f(2^{-j}x) \in \mathbf{V}_0, \forall j \in \mathbf{Z}$;
- (4) $\{\phi_l(x-k) : 1 \leq l \leq N, k \in \mathbf{Z}\}$ is *Reize*, for $\mathbf{C} = \{c_k\}_{k \in \mathbf{Z}} \in l^2(\mathbf{Z})^N$:

$$A \|c\|_{l^2(\mathbf{Z})^N}^2 \leq \left\| \sum_{n \in \mathbf{Z}} \sum_{k \in l^2} c_k^i \phi_l(x-k) \right\|_{L^2(\mathbf{R})}^2 \leq B \|c\|_{l^2(\mathbf{Z})^N}^2 \quad (5)$$

$0 < A \leq B < \infty$, we suppose that the vector scaling function $\Phi(x)$ is constituted by approximation of wavelet multi resolution. If

$$H_k, G_{k \in \mathbf{Z}}^i \in l^2(\mathbf{Z})^{N \times N}, \text{ satisfying}$$

$$\Phi(x) = \sum_{n \in \mathbf{Z}} H_n \Phi(Mx - k), \text{ then}$$

$$\Psi^{(i)}(x) = \sum_{n \in \mathbf{Z}} G_n^{(i)} \Phi(Mx - k) \text{ Where,}$$

$$\phi_{l,j,k}(x) = M^{j/2} \phi_l(M_j x - k),$$

$$\psi_{l,j,k}^{(i)}(x) = M^{j/2} \psi_l^{(i)}(M_j x - k)$$

Wavelet decomposition of multi-vector is defined as follows:

$$C_{j,k} = \langle f(x), \Phi_{j,k} \rangle = \frac{1}{\sqrt{M}} \sum_n H_n C_{j+1, Mk+n} \quad (6)$$

$$D_{j,k}^{(i)} = \langle f(x), \Psi_{j,k}^{(i)} \rangle = \frac{1}{\sqrt{M}} \sum_n G_n^{(i)} C_{j+1, Mk+n} \quad (7)$$

Reconstruction is

$$C_{j+1,k} = \frac{1}{\sqrt{M}} \sum_n (H_n C_{j, Mn+k} + \sum_{i=1}^{M-1} G_n^{(i)} D_{j, Mn+k}^{(i)}) \quad i = 0, \dots, N-1 \quad (8)$$

C. The Proposed Method based on Multi-band Vector Wavelet

In this paper, we present a multi-focus image fusion approach based on Multi-band vector wavelet transform and anisotropic diffusion arithmetic. Figure 2 describes

the Image fusion based on multi-band vector wavelet decomposition and reconstruction method. From this Figure, we can see there are two critical stages which are consisted in our approach: fusion and post-filtering (i.e., diffusion). In the first stage, a multi-band vector wavelet transform is used to obtain coefficients of high and low frequency bands, and then the fusion image. By analyzing we may find, obvious blocking effect always takes in fused image. Therefore, in the second stage, anisotropic diffusion arithmetic based on partial differential equations is used for post-processing to achieve the ultimately promoting image.

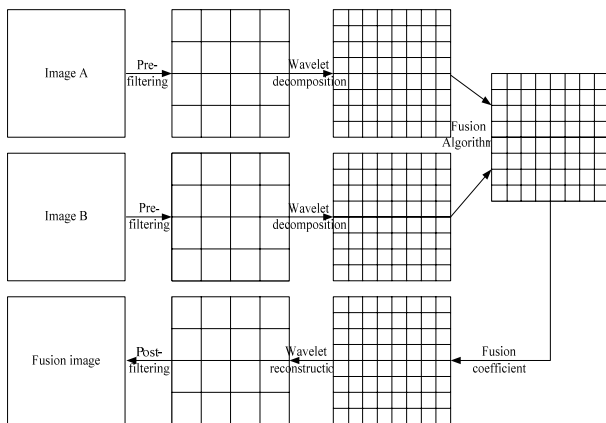


Figure 2. Image fusion based on our wavelet decomposition and reconstruction method

The specific flow chart of the proposed method is shown in Figure 3.

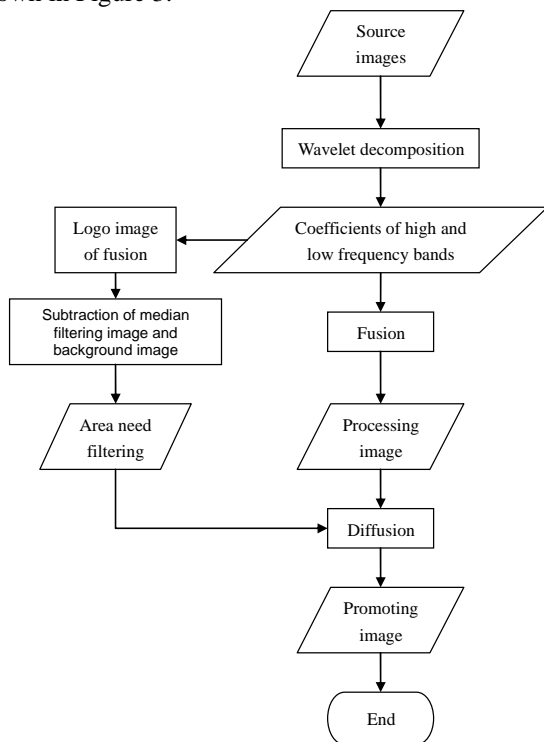


Figure 3. The flow chart of multi-focus image fusion approach by using the proposed method

Pixel-level multi-focus image fusion scheme is used in the proposed image fusion method. The common scheme for multi-band construction is always based on

conjugating filters in which calculation becomes more complicated with increasing order [13], M is set 4 in this paper. According to the Figure 2 and 3, the basic steps of proposed method are described as follows:

Step1. In the first step, all source images A and B to be fused is performed as a pre-filtering respectively. This process decomposes each source image into 16 sub-images, the upper left is the sub-image with low frequency signals, and the others are 15 sub-images with high frequency signals.

Step2. In the two groups of images, each of 16 sub-images is decomposed by vector wavelet with a multiplicity of 2. After then, 64 coefficients of low and high bands are obtained. For each source image, there are 64 decomposed image blocks. Among of these blocks, the 4 upper left are blocks with low frequency signals, and they will be fused with the same fusion rule. The rest of 60 blocks are blocks with high frequency signals, and will be fused with the same fusion rule.

Step3. In this step, the 64 coefficients from different source images will be fused with different rules as step 2 described, and then new 64 coefficients will be achieved. At last, an inverse WT is then performed on those new coefficients; thus, the fused image is constructed.

Step4. Based on the results of step 2, we calculate those pixels which need post-filtering.

Step5. We use anisotropic diffusion arithmetic based on partial differential equations in processing the fused image to eliminate the blocking effects (i.e., diffusion). After this process, the ultimately result image is obtained. The post-processing method is described in next section.

The fusion rules of high and low frequency bands that we have followed the method are described in Refs [14].

D. Post-processing Method

In wavelet based image fusion method, sharpness losing and blocking artifacts are always exhibited in the fused image, or in other words, there is edge degradation. These are the shortcomings of this type of fusion method. These problems occur frequently when images are processed in the frequency domain, such as the compression of images or video, the processing is generally performed on the macro blocks according to compression standards, so there usually are blocking effects [15]. For these images are achieved from the inverse transforms in the frequency domain, the general approach is that filter is performed on them to eliminate the blocking effects, e.g., in the H.264 code protocol of video compression, there is post-processing (i.e., filtering) on those images which are compression encoded and decoded in sequence. The insights from these studies motivated our post-processing researching approaches. We can employ similar measures to enhance the quality of the fused method based on WT methods.

At first, we will analyze the reasons why the edge degradation comes into being. By analyzing, we can find the reason is that image processing by artificially piecing out one source image to another in frequency domain results in the noises in time domain. The wavelet based algorithms usually have the clear edge blurred into a line which includes ghost effects. We carried out a

number of experiments with different fusion rules and scales. The experimental results indicate that it is impossible to eliminate the edge effects.

According to the above analysis, we tend to perform post-filtering by using nonlinear anisotropic diffusion for the goal of noise-removing, edge enhancement, remaining the original image's information. In the post-processing, we use the following diffusion equation for image filtering:

$$\partial u / \partial t = K \cdot g(|DG_{\sigma} * u|) |Du| \operatorname{div} \frac{Du}{|Du|}, u(0) = u_0 \quad (9)$$

where D represents gradient, div On behalf of divergence, G_{σ} is Gaussian template, $*$ is

$$\text{convolution, } g(s) = 1 - \frac{1}{1 + \frac{s^2}{k}}$$

$$\partial u / \partial t = K \cdot g(|DG_{\sigma} * u|) \frac{u_x^2 \cdot u_{yy} - 2 \cdot u_x \cdot u_y \cdot u_{xy} + u_y^2 \cdot u_{xx}}{u_x^2 + u_y^2} \quad (10)$$

In experiments, we set $\Delta t = 0.01$. Difference scheme is used in Equation of the first and second derivatives, the format of $u_x, u_y, u_{xx}, u_{yy}, u_{xy}$ is respectively:

$$\left(-\frac{1}{2} \quad 0 \quad \frac{1}{2}\right), \left(-\frac{1}{2} \quad 0 \quad \frac{1}{2}\right)^T, (1 \quad -2 \quad 1),$$

$$(1 \quad -2 \quad 1)^T, \begin{pmatrix} \frac{1}{4} & 0 & -\frac{1}{4} \\ 0 & 0 & 0 \\ -\frac{1}{4} & 0 & \frac{1}{4} \end{pmatrix}.$$

IV. EXPERIMENTAL RESULTS

In this section, several experimental results are introduced to show the effectiveness and the robustness of the proposed image fusion method. Assessment of image fusion performance of different methods studied in this paper is made quantitatively by using metrics that both employ subjective methods and objective methods.

A. Fusion Performance Evaluation

The fusion quality metrics include subjective and objective methods. Subjective method is always based on human visual perception. It gives direct comparisons. However, it is easily influenced by visual psychological factors. The effect of image fusion should be evaluated based on subjective vision and objective image quality assessment. A straightforward objective approach for fusion performance evaluation is to compare the fused image with a reference image. The commonly used methods include the root mean square error (RMSE), mean average error (MAE), the peak signal-to-noise ratio (PSNR), entropy (ENT), cross entropy (CE), mutual information (MI), correlation (CORR), and deference entropy (DE), to name a few [16]. In this paper, by using the first six means which are complemented basing on

human visual perception, the deference between the reference image and the fused one is calculated and serves as a measurement of the quality of the fused image. The expressions that correspond to the above six treatments which are selected are listed below.

(1) Root of mean square error (RMSE)

This metric can indicate how many errors the fused image conveys about the reference image. Hence, the lower the RMSE, the better the fused result.

$$RMSE = \sqrt{\frac{1}{MN} \sum_{i=1}^M \sum_{j=1}^N [R(i, j) - F(i, j)]^2} \quad (11)$$

Here M and N are the dimensions of the image.

(2) Mean error (ME)

ME indicates the dispersion degree between the fused image and the original image. With smaller MSE, there is less difference between them.

$$ME = \frac{1}{MN} \sum_{i=1}^M \sum_{j=1}^N |R(i, j) - F(i, j)| \quad (12)$$

(3) Peak signal to noise ratio (PSNR)

PSNR can reflect the quality of reconstruction. The larger the PSNR is, the less the image distortion is.

$$PSNR = 10 \cdot \lg \frac{L \times L}{\frac{1}{MN} \sum_{i=1}^M \sum_{j=1}^N [R(i, j) - F(i, j)]^2} \quad (13)$$

(4) Entropy (ENT)

ENT reflects the amount of information in fused image. The larger the EN is, the more information the image carries.

$$ENT = - \sum_{i=0}^{L-1} p_i \log_2 p_i \quad (14)$$

(5) Cross entropy (CE)

CE can reflect the difference between the two source images and the fused image. The smaller the CE is, the better fusion results are obtained.

$$CE = \sum_{i=0}^{L-1} p_i \log_2 \frac{p_i}{q_i} \quad (15)$$

(6) Mutual information (MI)

MI of two random variables is a quantity that measures the mutual dependence of the two variables. Hence, the larger the value of MI, the better the fusion result is.

$$MI(R, F) = \sum_{i=0}^{L-1} \sum_{j=0}^{L-1} h_{R,F}(i, j) \log_2 \frac{h_{R,F}(i, j)}{h_R(i) h_F(j)} \quad (16)$$

The meaning of the symbols used in the above equations is listed in Table 1.

B. Experimental Results

In order to compare the different wavelet based methods and our proposed method, and evaluate fused image quality, three 8-bit gray level images are used in all experiments: Lena figure, Cameraman figure and Michael & Lincoln figure. By using a 7×7 template, there is the

standard deviation of 5 with high intensity Gaussian blur and focus process, three groups of source images are generated focusing on the right and the left side image of these images respectively. We use a single wavelet 'db1', 'coif3', 'sym2', 'bior4.4' and 'dmey', four band in the wavelet 'db1', vector wavelet is used in 'ghm' dual wavelet and our method (i.e., 4 bands vector wavelet based on skew matrix) on these groups of source images.

The Experimental results are shown in Figure 4-9. To evaluate the performance of the proposed method objectively, the above six criteria are used. For these criteria (e.g., PSNR, ENT, MI), larger values indicate better fusion results, and for those other three criteria, just to the contrary, they are going in the opposite direction. The comparisons of these objective data are detailed shown in Table 2-7. From the results shown in Figure 4-6, Table 2-4, we can conclude that the proposed algorithm performs better on multi-focus image fusion than those other conventional wavelet-based methods on the overwhelming majority sides. However, carefully comparing the results in Figure 6-8, we can see that the fused results (i.e., fused image before diffusion) of the proposed method lose sharpness and exhibit prominent blocking artifacts, and then after the post-filtering, it can

be found that the result images after diffusion are more suitable for human visible perception. The detailed local images show these enhancements.

TABLE I.
THE NOTATION FOR ABOVE EQUATIONS

Symbols	Corresponding meanings
$R(i, j)$	Reference image
$F(i, j)$	Fused image
L	Maximum pixel value
p_i	Probability of value i of the reference image
q_i	Probability of value i of the fused image
$h_{R,F}(i, j)$	Normalized joint histogram of the reference image and the fused image
$h_R(i)$	Normalized marginal histogram of the reference image
$h_F(j)$	Normalized marginal histogram of the fused image



Figure 4. Comparison of the fusion for the Lena image. (a) focus on left, (b) focus on right, (c) fusion based on traditional wavelet method, (d) fusion based on our method.

TABLE II.
FUSION RESULTS COMPARISON FOR THE LENA IMAGE

Methods	PSNR	ME	RMSE	ENT	MI	CE
Wavelet 'db1'	33.2742	2.1487	5.5313	5.1480	3.3833	0.0113
Wavelet 'coif3'	33.0619	2.5354	5.6682	5.1429	2.9585	0.0122
Wavelet 'sym2'	33.4908	2.2215	5.3951	5.1419	3.1829	0.0109
Wavelet 'bior4.4'	33.8111	2.2844	5.1998	5.1386	3.0975	0.0142
Wavelet 'dmey'	32.5895	2.8570	5.9850	5.1469	2.7837	0.0121
Four-band wavelet	34.5750	2.3727	4.7620	5.1730	2.9370	0.0099
Vector wavelet	34.1623	1.9686	4.9937	5.1574	3.1808	0.0048
Our method	36.9678	1.3793	3.6153	5.1592	3.6536	0.0053

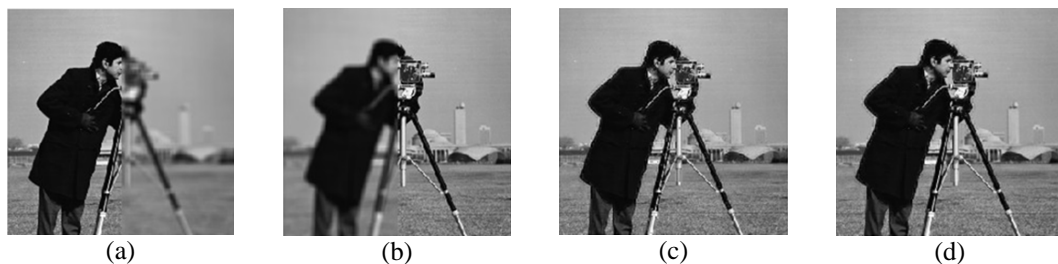


Figure 5. Comparison of the fusion for the Cameraman image (a) focus on left, (b) focus on right, (c) fusion based on traditional wavelet method, (d) fusion based on our method.

TABLE III.
FUSION RESULTS COMPARISON FOR THE CAMERAMAN IMAGE

Methods	PSNR	ME	RMSE	ENT	MI	CE
Wavelet 'db1'	30.8243	2.1935	7.3337	4.9173	3.3511	0.0233
Wavelet 'coif3'	30.6240	2.5575	7.5048	4.9122	2.9822	0.0241
Wavelet 'sym2'	31.3151	2.0971	6.9308	4.9010	3.2039	0.0164
Wavelet 'bior4.4'	31.0403	2.3179	7.1536	4.8980	3.0706	0.0195
Wavelet 'dmey'	30.2657	2.9266	7.8209	4.9356	2.8196	0.0358
Four-band wavelet	33.2384	2.2877	5.5542	4.9359	3.0357	0.0364
Vector wavelet	31.8081	2.0539	6.5484	4.8948	3.1001	0.0168
Our method	34.4235	1.4433	4.8458	4.9219	3.6100	0.0220



Figure 6. Comparison of the fusion for the Michael & Lincoln image
(a)focus on left, (b)focus on right, (c)fusion based on traditional wavelet method, (d)fusion based on our method.

TABLE IV.
FUSION RESULTS COMPARISON FOR Michael & Lincoln IMAGE

Methods	PSNR	ME	RMSE	ENT	MI	CE
Wavelet 'db1'	35.4921	1.7018	4.2849	5.2288	3.4872	0.0145
Wavelet 'coif3'	35.6863	1.8517	4.1901	5.2276	3.2390	0.0146
Wavelet 'sym2'	35.7746	1.6535	4.1477	5.2273	3.4217	0.0123
Wavelet 'bior4.4'	36.2248	1.6940	3.9382	5.2264	3.3442	0.0147
Wavelet 'dmey'	35.1796	2.1077	4.4418	5.2287	3.0735	0.0194
Four-band wavelet	37.0199	1.8088	3.5937	5.2314	3.1811	0.0214
Vector wavelet	35.9927	1.5836	4.0449	5.2261	3.3644	0.0087
Our method	39.0494	1.0891	2.8449	5.2341	3.7934	0.0133

The comparison of the fusion image before diffusion and after diffusion can be seen in figure 7-9 and in table 5-7.

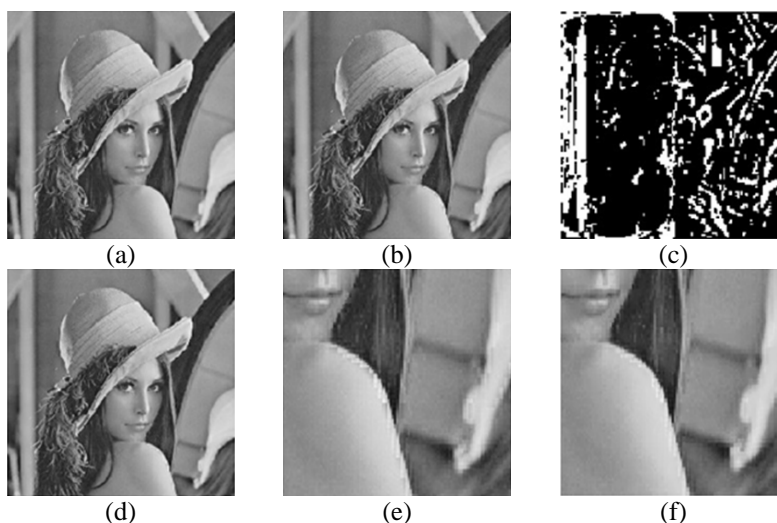


Figure 7. Comparison of filtering of Lena image. (a) standard image,(b) fusion image,(c) logo image,(d) image after diffusion,(e) details before diffusion ,(f) details after diffusion.

TABLE V.
COMPARISON OF THE FUSION IMAGE BEFORE DIFFUSION AND AFTER DIFFUSION (LENA IMAGE)

Methods	PSNR	ME	RMSE	ENT	MI	CE
Before diffusion	36.9678	1.3793	3.6153	5.1592	3.6536	0.0053
After diffusion	37.6306	1.4200	3.3497	5.1565	3.5428	0.0063

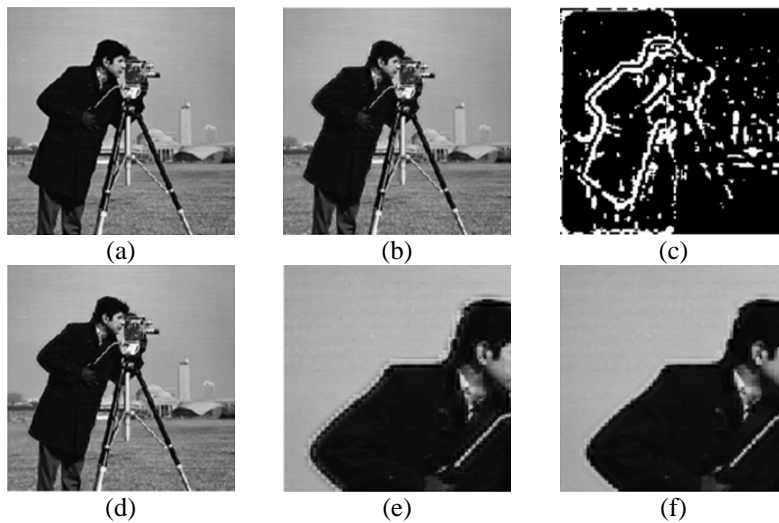


Figure 8. Comparison of filtering of Cameraman image. (a) standard image,(b) fusion image,(c) logo image,(d) image after diffusion,(e) details before diffusion ,(f) details after diffusion.

TABLE VI.
COMPARISON OF THE FUSION IMAGE BEFORE DIFFUSION AND AFTER DIFFUSION (Cameraman IMAGE)

Methods	PSNR	ME	RMSE	ENT	MI	CE
Before diffusion	34.4235	1.4433	4.8458	4.9219	3.6100	0.0220
After diffusion	35.1021	1.4038	4.4816	4.9140	3.5407	0.0222

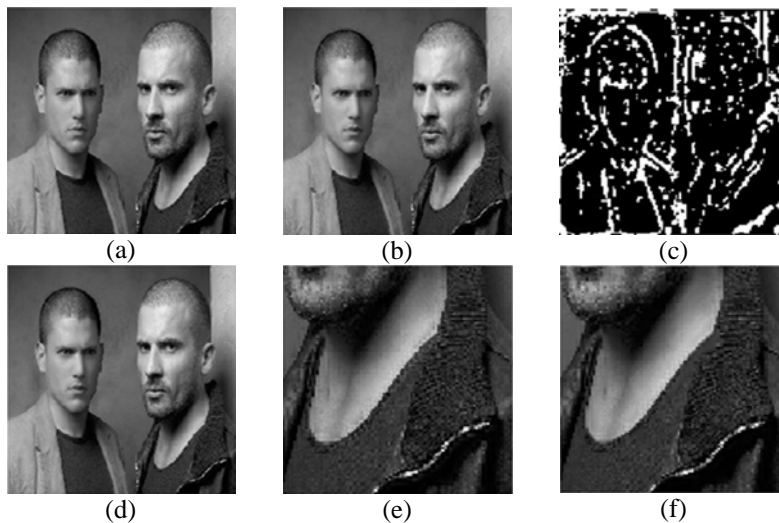


Figure 9. Comparison of filtering of Michael & Lincoln image. (a) standard image,(b) fusion image,(c) logo image,(d) image after diffusion,(e) details before diffusion ,(f) details after diffusion.

TABLE VII.
COMPARISON OF THE FUSION IMAGE BEFORE DIFFUSION AND AFTER DIFFUSION (Michael & Lincoln IMAGE)

Methods	PSNR	ME	RMSE	ENT	MI	CE
Before diffusion	39.0494	1.0891	2.8449	5.2341	3.7934	0.0133
After diffusion	39.3026	1.1306	2.7632	5.2327	3.7222	0.0133

V. DISCUSSION

The objective of image fusion is to combine information from multiple images of the same scene. The result of image fusion is a new image which is more suitable for human and machine perception or further image-processing tasks [17].

Previous researchers have formed comprehensive theory and method contribution in image fusion by long-

term work. This paper briefly describes those methods, and focuses on wavelet based methods.

Studies show that a simple single wavelet based method cannot meet the needs of the image fusion, multi-band wavelet and vector wavelet retain a lot of high quality properties, which include symmetry, compact support domain, orthogonality, short vanishing moments and so on. These properties shown the effectiveness in multi-focus image fusion by our experimental results,

especially the method based on multi-band multi-wavelets in the experiment achieving the best fusion results. Of course, the selection of wavelet is one of the most important factors in the role of the merits of image fusion method. Furthermore, it is still dependent on fusion operator selection. A variety of experiments on the fusion rules are compared, and finally we adopt the gradient energy maximum based regional fusion rule.

In image fusion, the role of the fusion rules is often more focused on, and the fusion process is stopped after image fusion is for improved image quality, this is not enough. The reason is that the image may be fused at the edge area, details of the highlights, etc. But the introduction of noise may be resulted and the image contrast may be changed. Therefore, the integration of image post-processing is essential. In this paper, the edge effect has been removed by using nonlinear anisotropic diffusion method; as well the experimental effect is very obvious.

What should be pointed out is that although the fusion results are much better, the real-time cannot be guaranteed, which in practice is a problem cannot be ignored. The main drawback, however, comes from that they are implemented with more complicated filter banks than the standard wavelet transforms, which leads to more computation. Due to the non-real-time, it will inevitably lead to background processing. The time consumed in the image fusion mainly lies in the multi-band multi-wavelet decomposition and reconstruction, as well as the diffusion equation iteration. We believe that with hardware performance improved, the algorithms optimization, real-time processing of image fusion will be resolved.

VI. CONCLUSIONS

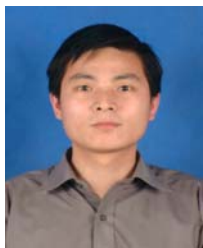
With the development of imaging technology, more and more digital image processing technologies are applied to some fields. However, by limiting the depth of field, it is difficult or impossible to make all the objects focused in the same scene. How to fuse the objects in order to make all the objects focused becomes imminent. Pixel-level fusion is the most basic fusion method, which is the basis of feature-level fusion and decision level fusion, and has been becoming a hot topic of research now. WT is a very popular technology which is used in pixel-level image fusion scheme. This paper provides a novel multi focus image fusion methods based on multi-band vector wavelet decomposition and reconstruction algorithm. Several WT based image fusion methods and the proposed wavelet based multi focus image fusion methods are evaluated by three images. Experiment results show the proposed techniques can provide better performance than other fusion measures. Furthermore, using anisotropic diffusion arithmetic based on partial differential equations, a post-filtering method is applied in the proposed method. It can eliminate the blocking effects in the fused image effectively, and improve the visibility quality which is assessed by human visual perception.

ACKNOWLEDGMENT

This work is supported in part by the National Natural Science Foundation of China Grant No.40806011, by the JiangSu Natural Science Foundation under Grant BK20082140, and by the Huaihai Institute of Technology Natural Science Foundation under Grant Z2009013, and by the key disciplines in computer application Construction Foundation of JiangSu.

REFERENCES

- [1] W. Huang and Z. Jing, "Evaluation of focus measures in multi-focus image fusion," *Pattern Recognition Letters*, vol. 28, pp. 493-500, 2007.
- [2] B. Yang and S. Li, "Multi-focus image fusion based on spatial frequency and morphological operators," *Chinese Optics Letters*, vol. 5, pp. 452-453, 2007.
- [3] V. Aslantas and R. Kurban, "Fusion of multi-focus images using differential evolution algorithm," *Expert Systems with Applications*, 2010.
- [4] H. Jiang and Y. Tian, "Fuzzy image fusion based on modified Self-Generating Neural Network," *Expert Systems with Applications*, 2011.
- [5] J. J. Lewis, et al., "Pixel-and region-based image fusion with complex wavelets," *Information Fusion*, vol. 8, pp. 119-130, 2007.
- [6] Y. Lu, et al., "A multi-focus image fusion based on wavelet and region detection," 2007, pp. 294-298.
- [7] J. Peter and H. Edward, "The Laplacian pyramid as a compact image code," *IEEE Transactions on Communications*, vol. 31, pp. 532-540, 1983.
- [8] P. J. Burt, "A gradient pyramid basis for pattern-selective image fusion," *Proceedings of the Society for Information Display*, p. 467-470, 1992.
- [9] Z. Zhang and R. S. Blum, "A categorization of multi scale decomposition-based image fusion schemes with a performance study for a digital camera application," *Proceedings of the IEEE*, vol. 87, pp. 1315-1326, 1999.
- [10] W. Shi, et al., "Wavelet-based image fusion and quality assessment," *International Journal of Applied Earth Observation and Geoinformation*, vol. 6, pp. 241-251, 2005.
- [11] Goodman T.N.T., Lee S.L. and Tang W.S. Wavelet wandering subspaces. *Trans. Amer. Math. Soc.*1993, 338(2):639-654
- [12] G. Piella, "A general framework for multiresolution image fusion: from pixels to regions," *Information Fusion*, vol. 4, pp. 259-280, 2003.
- [13] P. Steffen, et al., "Theory of regular M-band wavelet bases," *Signal Processing, IEEE Transactions on*, vol. 41, pp. 3497-3511, 1993.
- [14] S. Huang, Y. Yang, "An Effective Scheme of Wavelet Coefficients for Multiresolution Image," *Advanced Materials Research* Vols. 108-111pp. 730-735, 2010
- [15] Chan T.F. and Esedoglu S. Aspects of total variation regularized L1 function approximation. *SIAM J. Appl. Math.* vol. 65(5):1817-1837,2005.
- [16] Y. Wang and B. Lohmann, "Multisensor image fusion: concept, method and applications," *Univ. Bremen, Bremen, Germany, Tech. Rep.*, 2000.
- [17] G. Pajares and J. Manuel de la Cruz, "A wavelet-based image fusion tutorial," *Pattern Recognition*, vol. 37, pp. 1855-1872, 2004.
- [18]



Yihua Lan received his Ph.D. degree in Computer Science from the School of Computer Science and Technology, Huazhong University of Science and Technology, Wuhan(HUST) in 2011, now he held teaching and research positions at School of Computer Engineering, Huaihai Institute of Technology (HHIT), Jiangsu, China. His research areas are image processing and analysis. His research interests include PDE methods for image processing, iterative methods, Krylov subspace methods, optimization algorithms, and artificial intelligence.



Haozheng Ren received the M.S.degree in computer engineering, China, in 2006, from the Lanzhou University of Technology. She is currently a teacher of the School of Computer Engineering, Huaihai Institute of Technology, where she has been an Instructor since 2008. Her research interests include PDE methods for image processing, iterative methods, Krylov subspace methods, and

parallel algorithms.



Yong Zhang received the M.S.degree in in School of computer science, SuZhou University in 2007, China. His M.S. subject is digital image processing. He held teaching and researching positions at the School of Computer Engineering, Huaihai Institute of Technology, where he has been an instructor. His research interests include image processing and machine vision.



Chih-cheng Hung is professor of Computer Science at Southern Polytechnic State University, USA. He received his B.S. in business mathematics from Soochow University, and his M.S. and Ph.D. in Computer Science from the University of Alabama in Huntsville. His research interests include multi-spectral image processing and analysis, computational intelligence, and pattern recognition.